



## Poster Abstracts

68<sup>th</sup> Lindau Nobel Laureate Meeting  
24 – 29 June 2018



LINDAU  
NOBEL LAUREATE  
MEETINGS

## POSTER OVERVIEW

#	T	First Author	Title
<b>Infection and Immunity</b>			
1	C	Neta Varsano	Characterization of Cholesterol Crystal Formation in Macrophage Foam Cells. Relevance to Atherosclerosis
2	B	Mircea-Andrei Sandu	Secretion of an intracellular protein is protective after myocardial ischemia-reperfusion injury
3	A	Sebastian Beck	The Importin- $\alpha$ 7 Interactome as a Platform to Study Molecular Mechanisms Involved in Influenza A Virus Host Switch
4	B	Mathew Stracy	How do persister cells survive antibiotic treatment?
5	C	Cornelius Thaiss	A network of protection across tissues drives vaccine efficiency
6	A	Irini Evnouchidou	The function of IRAP+ endosomes in T cells
7	B	Ryuta Uraki	Zika virus infects testes, leading to male to female sexual transmission.
<b>Genetics</b>			
8	A	Mohamed El-Brolosy	Mutant mRNA decay confers genetic robustness to mutations through triggering transcriptional upregulation of related genes.
9	C	Maude Giroud	Non-coding RNAs are important regulators of adipocyte plasticity
10	B	Rachel Bayley	A novel role for chromatin dynamics in maintaining genome stability
11	C	Johanna Magdalena Schmidt	Exome sequencing in human bladder exstrophy and knockdown studies in zebrafish implicate SLC20A1 as candidate gene and a major regulator of urinary tract development
<b>Cell Biology</b>			
12	B	Scott Berry	Transcriptome adaptation to cell shape
13	C	Miaohui Hu	Pore Architecture and Gating Mechanism of TRIC Channels
14	A	Shireen Mentor	Morphologically mapping the development of the blood-brain barrier using high resolution electron microscopy
15	C	Kapil Ramachandran	Coupled protein synthesis and degradation through a neuronal 20S plasma membrane proteasome complex
16	A	Toru Hiratsuka	Pulsing and propagating features of ERK MAPK signal in mammalian skin.
<b>Cancer</b>			
17	B	Stella Paffenholz	Dissecting the Contribution of Recurrent p53 Gain-of-Function Mutations to Pancreatic Tumorigenesis

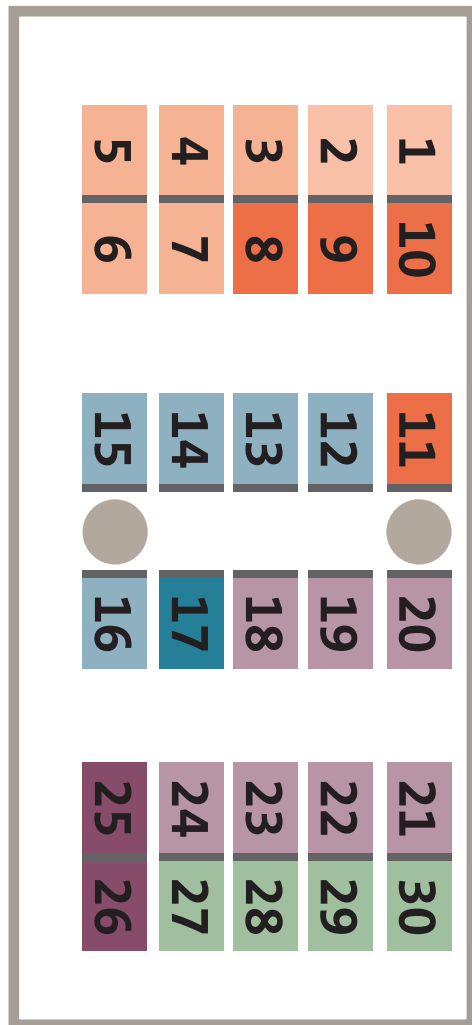
## POSTER OVERVIEW

#	T	First Author	Title
<b>Technology</b>			
18	C	Dimitra Pouli	In vivo, label-free evaluation of mitochondrial dynamics in human skin enables non-invasive classification of malignant skin lesions.
19	A	Qiaoshi Lian	AIM2 activation causes intestinal toxicity in chemotherapy
20	B	Aditi Mehta	Inhalable nanoparticles for in vivo genome editing mediated by crispr-cas9 delivery for undruggable KRAS driven lung cancers
21	A	Yunus Alapan	Microengineering Approaches to Red Blood Cell-Based Diagnostics and Drug Delivery
22	C	Katharina Martini	Dynamic MRI as outcome predictor for Lung Volume Reduction Surgery in patients with severe emphysema
23	B	Florian Siegerist	Three-dimensional structured illumination microscopy as a novel diagnostic tool for nephrotic kidney diseases
24	A	Nicholas Cohrs	A Soft Total Artificial Heart – 3D-Printing and Softness for More Physiological Implants
<b>Structural Biology</b>			
25	B	Alexandra Walls	Structural characterization of coronavirus fusion proteins
26	A	Daniel Stöppler	Insight into Small Molecule Binding to the Neonatal Fc Receptor by X-ray Crystallography and 100 kHz Magic-Angle-Spinning NMR
<b>Neurobiology</b>			
27	C	Stefan Frässle	Inferring whole-brain effective connectivity
28	B	Tanja Müller	Tired of working: The impact of effortful exertion on brain and behaviour
29	C	Takato Honda	Investigation of Sleep/Wake Regulatory Mechanisms by Analysis of the Sik3 Gene Identified Through Forward Genetics
30	A	Maximilian Bauer	Functional impairment of cortical astrocytes in ALS-transgenic mice

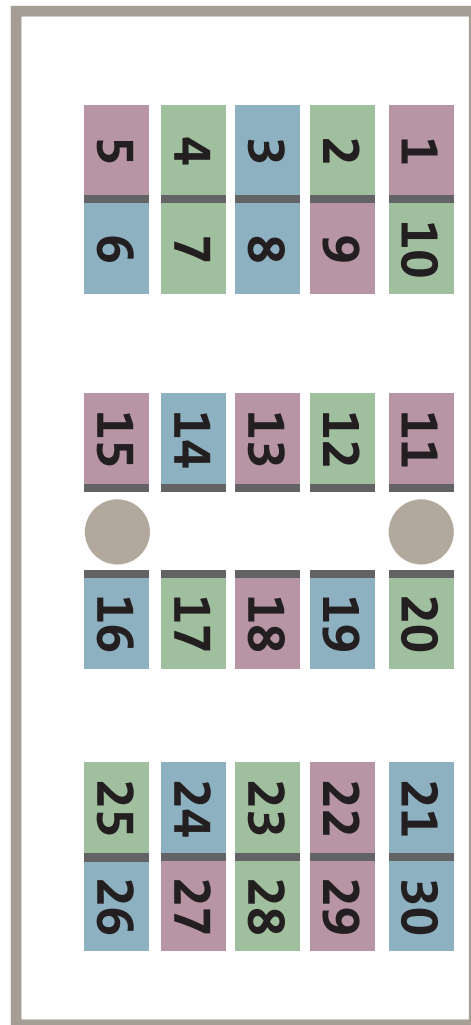
### Poster Presentation Time Slots

<b>A</b>	Tuesday, 26 June 2018	13.30-14.30
<b>B</b>	Wednesday, 27 June 2018	13.30-14.30
<b>C</b>	Thursday, 28 June 2018	13.30-14.30

## POSTER PLAN



**Colored by Topic Area**  
See preceding pages for details.



**Colored by Presentation Time**

<b>A</b>	Tuesday, 26 June 2018	13.30-14.30
<b>B</b>	Wednesday, 27 June 2018	13.30-14.30
<b>C</b>	Thursday, 28 June 2018	13.30-14.30

## INFORMATION

### Posters

The posters will be on display in the basement of the Inselhalle from Monday to Thursday.

### Poster Presentations

The poster authors will be available at their posters to present and explain their posters during the times stated on the left page.

### Poster Flashes

The research presented on the poster will also be presented in a 90 minute poster flash session, where every presenter may show a maximum of two slides and has two minutes of time. The poster flash takes place on Monday at 17.00 hrs at the city theatre. Posters will be presented in the order shown on the preceding pages.

### Poster Awards

This brochure includes a voting sheet. Please put your voting sheet in one of the boxes or return it to the Young Scientists Desk by Thursday, 28 June 2018, 16.30 hrs, at the latest. The winners will be announced during the boat trip on Friday, 29 June 2018.

### Poster Setup

- All poster walls have a useable area of 120 cm width and 150 cm height. We recommend posters in size A0 (84,1 x 118,9 cm).
- Posters may be set up on Sunday, 24 June 2018.
- Posters have to be provided by the authors; no on-site printing is available. Tape and fixing pins are available in the poster area.
- Posters have to be placed on designated walls – please refer to the poster number published in this brochure.
- Posters have to be removed by the presenters immediately after the poster session on Thursday, i.e. between 14.30 – 17.00 hrs. Posters not removed will not be stored.

## Characterization of Cholesterol Crystal Formation in Macrophage Foam Cells. Relevance to Atherosclerosis

**Neta Varsano**<sup>†</sup>, Fabio Beghis, Nadav Elad<sup>‡</sup>, Eva Pereiro<sup>§</sup>, Tali Dadosh<sup>‡</sup>, Iddo Pinkas<sup>‡</sup>, Ana J Perez-Berna<sup>||</sup>, Xueting Jin<sup>⊥</sup>, Howard S. Kruth<sup>⊥</sup>, Leslie Leiserowitz<sup>#</sup>, and Lia Addadi<sup>†</sup>

<sup>†</sup>Department of Structural Biology, <sup>‡</sup>Department of Chemical Research Support, and <sup>#</sup>Department of Materials and Interfaces, Weizmann Institute of Science, Rehovot, 76100, Israel <sup>§</sup> Università Degli Studi Di Milano, Department of Chemistry, I-20122 Milano, Italy <sup>||</sup> ALBA Synchrotron Light Source, MISTRAL Beamline—Experiments Division, 08290 Cerdanyola del Valles, Barcelona, Spain <sup>⊥</sup> Experimental Atherosclerosis Section, National Heart, Lung, and Blood Institute, National Institutes of Health, Bethesda, Maryland 20892-1422, United States

Accumulation of cholesterol in the blood vessel walls is a prominent feature of atherosclerosis (1), a major precursor of most cardiovascular diseases. Cholesterol crystal deposition is a crucial stage in the pathological cascade involving cell death, increased inflammatory response and plaque disruption (2).

We set out to study the early events involved in the onset of the irreversible step of crystal nucleation. We incubated macrophage cells with acLDL particles for different time lengths and followed the cholesterol segregation process by using an antibody that identifies the newly formed cholesterol crystals (3). Their direct imaging can be achieved by using a recently developed correlative method that combines cryo soft X-ray tomography (cryo-SXT) with stochastic optical reconstruction microscopy (STORM) (4).

At early incubation stages with acLDL, we identified small (200 nm) cholesterol crystal plates that are located at the plasma membrane interface of the cells. The cholesterol plates match in their morphology those of the commonly observed cholesterol monohydrate triclinic structure (2) and may subsequently assemble into large aggregates inside the cell membrane (5). These observations strengthen our hypothesis that 3D cholesterol crystals grow from 2D cholesterol membrane domains, as they do in supported lipid bilayers (6).

When cells are incubated with acLDL for longer time periods, large rod-like cholesterol crystals form in intracellular locations. The crystals are located inside the cell volume with no obvious association to the plasma membrane. Their elongated rod-like morphology is also similar to that of the crystals isolated from atheromas (7). Using cryo-transmission electron microscopy (cryo-TEM) and cryo-electron diffraction (cryo-ED), we show (5) that the crystal structure of the rods corresponds to that of monoclinic cholesterol monohydrate (8). These monoclinic crystals form with unusual hollow cylinder or helical architecture (5), similar to those formed when cholesterol pathologically crystallizes from bile (9). To the best of our knowledge, this is the first identification of the monoclinic polymorph in atherosclerosis-related models. We believe that our findings, besides explaining the different crystal morphologies that appear in human plaques, may potentially serve for elucidating the mechanisms by which cholesterol crystallizes in atherosclerotic lesions.

1. Kruth, H. S. (1984). *Am. J. Pathol.*, 114(2), 201.
2. Small, D. M. (1988). George Lyman Duff memorial lecture. *Arterioscler. Thromb. Vasc. Biol.*, 8(2), 103-129.
3. Perl-Treves D, Kessler N, Izhaky D, Addadi L. (1996). *Chem Biol.*, 3, 567
4. Varsano, N., Dadosh, T., Kapishnikov, S., Pereiro, E., Shimoni, E., Jin, X. Kruth H. S., Leiserowitz L. & Addadi, L. (2016). *J. Am. Chem. Soc.*, 138(45), 14931-14940
5. Varsano N., Beghi F., Elad N., Pereiro E., Dadosh T., Pinkas I., Perez-Berna A.J., Jin X., Kruth S.H., Leiserowitz L., & Addadi L., *Proc. Natl. Acad. Sci.*, under review.
6. Varsano, N., Fargion, I., Wolf, S. G., Leiserowitz, L., & Addadi, L. (2015). *J. Am. Chem. Soc.*, 137(4), 1601-1607.
7. Kruth, H. S. (2001). *Curr. Mol. Med.*, 1(6), 633-653.
8. (a) Solomonov, I., Weygand, M. J., Kjaer, K., Rapaport, H., & Leiserowitz, L. (2005). *Biophys. J.*, 88(3), 1809-1817. (b) Rapaport, H., Kuzmenko, I., Lafont, S., Kjaer, K., Howes, P. B., Als-Nielsen, J., Lahav M. & Leiserowitz, L. (2001). *Biophys. J.*, 81(5), 2729-2736.
9. Weihs, D., Schmidt, J., Goldiner, I., Danino, D., Rubin, M., Talmon, Y., & Konikoff, F. M. (2005). *J. Lipid Res.*, 46(5), 942-948.

## Secretion of an intracellular protein is protective after myocardial ischemia-reperfusion injury

Sandu MA<sup>1</sup>, Korf M<sup>1</sup>, Reboll MR<sup>1</sup>, Polten F<sup>1</sup>, Wang Y<sup>1</sup>, Bauersachs J<sup>1,2</sup>, Wollert KC<sup>1,2</sup>

<sup>1</sup> Division of Molecular and Translational Cardiology, Hannover Medical School

<sup>2</sup> Department of Cardiology and Angiology, Hannover Medical School  
Carl-Neuberg-Straße 1, 30625 Hannover, Germany

**BACKGROUND:** The modest restoration of heart function attributed to myocardial infarction (MI) patients receiving intracoronary infusion of bone marrow mononuclear cells (BMC) proved to be the milestone of further research, which concluded that paracrine signaling of bone marrow progenitors that home to the ischemic tissues may promote cardiac healing after injury. Driven by the concept that BMC progenitors secrete cardioprotective chemokines during heart ischemia, our group isolated a fraction of CXCR4<sup>high</sup> BMC from 6 patients with MI, and identified, through an extensive bioinformatic secretome analysis, a peptide provisionally called Factor36 (F36) with angiogenic and cardiomyocyte-protective properties, whose function in the cardiovascular field was previously unknown.

**METHODS:** We investigated the angiogenic potential of F36 in human coronary artery endothelial cells and infarcted mouse heart explants. The antiapoptotic effects of the peptide were tested in cultured neonatal rat ventricular cardiomyocytes undergoing simulated ischemia (3h) and reperfusion (1h) injury. We defined the F36 cellular sources and cardiac expression pattern using wild-type mice subjected to transient coronary artery ligation. Furthermore, we explored the therapeutic potential of recombinant F36 delivered via osmotic minipumps in FVB/N mice subjected to ischemia-reperfusion injury (IRI).

**RESULTS:** F36 enhanced the proliferation and migration of cultured endothelial cells through an ERK-mediated upregulation of CCL2 (chemokine C-C motif ligand 2). Moreover, F36 promoted in a CCL2-dependent manner the outgrowth of endothelial cells from infarcted mouse heart explants, thus actively contributing to the healing process after the development of injury. Complementary to its proangiogenic effects, F36 improved the cell metabolism and reduced the enzymatic activity of caspase-3 and caspase-7 in cardiomyocytes undergoing IRI. F36 protein levels were massively increased in the infarcted region of the left ventricle and in the circulation of wild-type mice subjected to IRI, reaching a peak at the third postoperative day. Bone marrow- and spleen-derived monocytes and neutrophils were identified as the main cell sources to express F36 in the infarcted heart at 3 days after reperfusion. IRI-subjected FVB/N mice treated with recombinant F36 displayed enhanced cardiac contractility and attenuated ventricular remodeling compared to saline-infused control mice. According to histology data, F36 protein therapy reduced infarct size, attenuated scar formation, and increased the capillary density in the border zone of the infarcted territory.

**CONCLUSION:** We identified F36 as a previously unknown angiogenic and cardioprotective protein that is produced by bone marrow- and spleen-derived monocytes and neutrophils as part of an endogenous adaptive response that can be enhanced therapeutically to protect and repair the heart after MI.



## The Importin- $\alpha$ 7 Interactome as a Platform to Study Molecular Mechanisms Involved in Influenza A Virus Host Switch

Sebastian Beck<sup>1</sup>, Julia Hoffmann<sup>1</sup>, Swantje Thiele<sup>1</sup>, Victoria Sohst<sup>2</sup>, Friedrich Buck<sup>3</sup>,  
Thorsten Klingen<sup>4</sup>, Alice McHardy<sup>4</sup>, Stephanie Stanelle-Bertram<sup>1,5</sup> and Gülsah Gabriel<sup>1,5</sup>

<sup>1</sup> Heinrich Pette Institute, Leibniz Institute for Experimental Virology, Martinistrasse 52, 20251 Hamburg, Germany; <sup>2</sup> Research Center Borstel, Parkallee 1-40, 23845 Sülfeld, Germany;

<sup>3</sup> University Hospital Hamburg-Eppendorf, Martinistrasse 52, 20246 Hamburg, Germany;

<sup>4</sup> Helmholtz Centre for Infection Research, Inhoffenstrasse 7, 38124 Braunschweig, Germany;

<sup>5</sup> Center for Cell and Structural Biology in Medicine, University of Lübeck,  
Ratzeburger Allee 160, 23562 Lübeck, Germany.

Influenza A virus (IAV) adaptation from animal-to-man is orchestrated by a complex interplay of viral proteins with various cellular factors. We have shown in the past that importin- $\alpha$ 7, a component of the cellular nuclear import machinery, acts as a positive regulator of human-type polymerase activity thereby facilitating IAV interspecies transmission [1].

In order to elucidate importin- $\alpha$ 7 interacting cellular networks that might promote IAV replicative fitness in human cells, here, we performed an unbiased mass spectrometry approach. We identified several importin- $\alpha$ 7 interacting cellular proteins that have been previously linked to IAV infections, including DDX21, NCBP1 and ANP32A. Since ANP32A was only recently shown to be involved in IAV host switch [2], we investigated this interaction in more detail. Using various biochemical analyses we could show that ANP32A is imported into the nucleus via its C-terminal nuclear localization signal (NLS) in an importin- $\alpha$ 7 dependent manner. In order to determine whether the positive-regulatory function of importin- $\alpha$ 7 is mediated by ANP32A, we further established an importin- $\alpha$  overexpressing vRNP reconstitution assay in mammalian cells. Upon knockdown of ANP32A, importin- $\alpha$ 7 retains its effect on human-type polymerase activity. Likewise, ANP32A positively regulates viral polymerase activity in importin- $\alpha$ 7 silenced cells. Interestingly, this effect is also independent of its NLS sequence, suggesting a cytoplasmic function of ANP32A.

In conclusion, we propose that importin- $\alpha$ 7 and ANP32A unfold differential mode of actions in promoting viral polymerase activity in human cells. This knowledge will help to increase our current understanding of viral adaptation and to identify novel targets for therapeutic intervention.

[1] Hudjetz, B. and G. Gabriel, PLoS Pathog, 2012. 8(1): p. e1002488.

[2] Long, J.S., et al., Nature, 2016. 529(7584): p. 101-4.

## How do persister cells survive antibiotic treatment?

Mathew Stracy and David Sherratt

Department of Biochemistry, University of Oxford  
South Parks Rd, Oxford, OX1 3QU, UK

Many bacterial infections cannot be cured, even when caused by a pathogen that is not resistant to antibiotics. Central to this effect is the presence of a small population of cells called persisters, which enter a dormant state that protects them from bactericidal antibiotics. After treatment finishes, the surviving persisters can resume growth causing recurrent and chronic infections. Eradicating persisters is a crucial step towards treating these chronic infections, but little is known about the exact mechanisms by which they survive antibiotic treatment.

A variety of different pathways can trigger persistence. For example, stochastic expression of the HipA toxin causes inhibition of protein synthesis, driving cells into dormancy [1]. Alternatively, fluoroquinolone antibiotics induce expression of TisB, a membrane acting peptide, which depletes ATP levels leading to persistence [2]. It remains to be established if different pathways lead to similar final cell states, and if these convey the same levels of tolerance to different antibiotics.

To help answer these questions, we have developed a series of assays using super-resolution microscopy combined with single-particle tracking (sptPALM [3]) of the target proteins of three major classes of antibiotics (fluoroquinolones,  $\beta$ -lactams, and rifampicin). By directly measuring changes in the mobility of the antibiotic targets, we can test if the drugs are performing their function in individual *Escherichia coli* cells [4, 5]. Combining this technique with time lapse microscopy allows us to compare susceptible cells with cells which survive the treatment.

Our results show that the physiology of persister cells is dependent on the pathway which triggered dormancy, and that different persister states protect against killing via different mechanisms. For example, in susceptible cells ciprofloxacin binds to DNA gyrase during its catalytic cycle, and prevents ligation reactions leading to accumulation of double-stranded DNA breaks and cell death. In cells with inhibited protein synthesis, we found that ciprofloxacin was still active against gyrase, but DNA break repair was enhanced, leading to increased survival. In contrast, cells with depleted ATP were protected from killing due to decreased catalytic activity of DNA gyrase. Furthermore, our results suggest that different persister states can become susceptible to antibiotics at different time points after revival.

[1] E. Rotem et al. PNAS **107**, 12541–6 (2010).

[2] T. Dörr et al. PLoS Biol **8**, e1000317 (2010).

[3] S. Manley et al. Nature methods **5**, 155–157 (2008).

[4] M. Stracy et al. PNAS **112**, 201507592 (2015).

[5] M. Stracy et al. Nature communications **7**, 12568 (2016).

## A network of protection across tissues drives vaccine efficiency

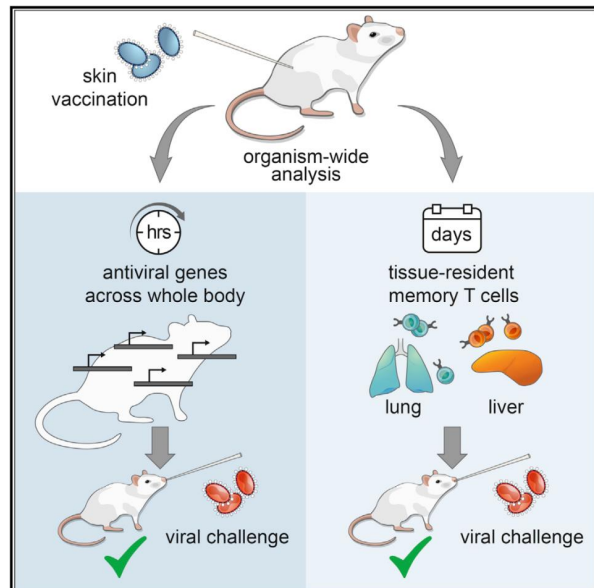
Cornelius C. Thaïss, Motohiko Kadoki, Ashwini Patil, Nicolas Chevrier

Faculty of Arts & Sciences Center for Systems Biology, Harvard University, Cambridge, MA 02138, USA;

Ludwig Maximilian University of Munich, 80539 Munich, Germany

A fundamental challenge in immunology is to decipher the principles governing immune responses at the whole-organism scale. We have used a comparative infection model and observed immune signal propagation within and between organs to obtain a dynamic map of immune processes at the organism level. We uncovered two inter-organ mechanisms of protective immunity mediated by soluble and cellular factors. First, analyzing ligand-receptor connectivity across tissues revealed that type I interferons trigger a whole-body antiviral state, protecting the host within hours after skin vaccination. Second, combining parabiosis, single-cell analyses, and gene knockouts, we uncovered a multi-organ web of tissue-resident memory T cells that functionally adapt to their environment to stop viral spread across the organism. These results have implications for manipulating tissue-resident memory T cells through vaccination and open up new lines of inquiry for the analysis of immune responses at the organism level [1].

1. Kadoki, M., et al., *Organism-Level Analysis of Vaccination Reveals Networks of Protection across Tissues*. Cell, 2017. **171**(2): p. 398-413 e21.



## The function of IRAP+ endosomes in T cells

Irini Evnouchidou<sup>1</sup>, Pascal Chappert<sup>2</sup>, Samira Benadda<sup>1</sup>, Andres Zucchetti<sup>3</sup>, Mariacristina De Luca<sup>1</sup>, Mirjana Weimershaus<sup>1</sup>, Marcelle Bens<sup>1</sup>, Peter van Ender<sup>2</sup>, Pierre Guernonprez<sup>1</sup>, Claire Hivroz<sup>3</sup>, David Gross<sup>2</sup>, Loredana Saveanu<sup>1</sup>

1. INSERM U1149, CRI, Université Paris Diderot, 16 rue Henri Huchard, 75018, Paris, France.

2. INSERM U1151, CNRS U8253, Université Paris Descartes, 149 rue de Sèvres, 75015, Paris, France.

3. INSERM U932, Institut Curie, Paris Sciences and Lettres Research University, 26 rue d'Ulm, 75005, Paris, France.

The activation of T lymphocytes is a complex phenomenon and the molecular mechanisms that are implicated are not completely known. T lymphocytes form an immunological synapse (IS) with cells infected by pathogens or cancer cells, after recognition of MHC/antigens by the T cell receptor (TCR). TCR cell surface expression, its internalization and its recycling are important for T cell activation. However, the factors controlling TCR recycling and endocytosis are poorly described, probably because of the complexity of the endocytic system. The molecules involved in T cell activation (TCR chains, Lck, LAT, etc) are recruited to the IS from distinctive endosomes, suggesting that regulated endosomal trafficking is mandatory for TCR activation. Among the endosomal populations displaying a regulated trafficking are the slow recycling, cell-specific regulated endosomes (SRSE) described by the aminopeptidase IRAP (Insulin Responsive AminoPeptidase). Initial studies showed that the trafficking of these endosomes is regulated by the insulin receptor in adipocytes and by FcRs in mast cells and dendritic cells (DCs). We observed that SRSE are well expressed in T cells and colocalize partially with Rab4, a small GTPase reported to contribute to TCR recycling. Prompted by this observation, we decided to investigate their function in T cell activation.

Using a model antigen that is presented in an IRAP-independent manner by DCs, we observed that IRAP KO mice show a deficiency in CD8+ T cell priming. Preliminary experiments using mice that are deficient for IRAP only in T cells (IRAP-lox-lox mice crossed with Lck-cre mice) revealed a decreased effector CD8+ T cell number 14 days after immunization. Since IRAP+ endosomes had never been studied before in T cells, we proceeded to the characterization of this compartment by immunoprecipitations and immunofluorescence not only in mouse transgenic OTI cells but also in the Jurkat human T cell line. We demonstrated that IRAP colocalizes and coimmunoprecipitates with Rab4 and with CD3z, the limiting TCR component for signal transduction. In order to study IRAP's impact on IS formation, we formed IS between Jurkat and Raji B cells loaded with the SEE (staphylococcal enterotoxin E) superantigen. We demonstrated that Jurkat IRAP KO T cells present a defect in IL-2 production. The same defect is observed using a melanoma antigen, the MART-1 peptide, with Jurkat that express a MART-1 specific TCR. In addition, the absence of IRAP inhibits the polarized recruitment of Lck and pZAP70 to the synapse and leads to a strong reduction in TCR signaling as well as in the TCR-ZAP70 interaction measured by FRET-FLIM (Fluorescence Resonance Energy Transfer-Fluorescence Lifetime Imaging Microscopy). According to our preliminary results, we suggest that TCR recycles via IRAP endosomes and that this recycling is essential for the engagement of the TCR-dependent signaling pathways. Our results will help to the understanding of molecular mechanisms implicated in T cell activation, a crucial step of the adaptive immune response on which is based the organism's defense towards pathogens and tumors.

## Zika virus infects testes, leading to male to female sexual transmission.

Ryuta Uraki<sup>1</sup>, Kellie Ann Jurado<sup>1</sup>, Jesse Hwang<sup>1</sup>, Laura J. Yockey<sup>1</sup>, Sarah Householder<sup>1</sup>, Andrew K. Hastings<sup>1</sup>, Klara Szigeti-Buc<sup>1</sup>, Robert J. Homer<sup>1,2</sup>, Tamas Horvath<sup>1</sup>, Akiko Iwasaki<sup>1,3</sup>, and Erol Fikrig<sup>1,3</sup>

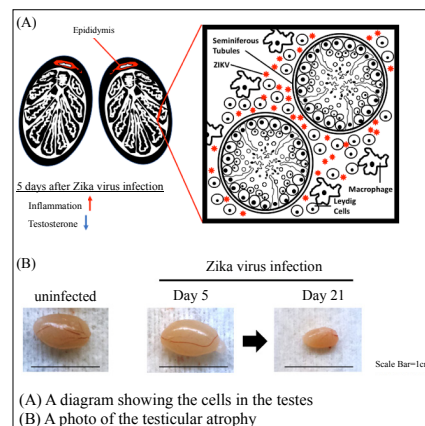
<sup>1</sup>Yale University School of Medicine, 300 Cedar St., New Haven, CT 06520, USA. <sup>2</sup>VA Connecticut Healthcare System Pathology and Laboratory Medicine Service, 950 Campbell Ave. West Haven, CT, 06516, USA. <sup>3</sup>Howard Hughes Medical Institute, 4000 Jones Bridge Road, Chevy Chase, MD, 20815, USA

Zika virus (ZIKV) is an emerging mosquito-borne flavivirus that has recently been found to cause fetal infection and neonatal abnormalities, including microcephaly and neurological dysfunction [1]. ZIKV persists in the semen months after the acute viremic phase in humans [2]. To further understand this presentation, we infected mice lacking the type I interferon receptor (*Ifnar1*<sup>-/-</sup>) via subcutaneous injection of a pathogenic but nonlethal ZIKV strain. ZIKV antigens were strongly detected in the interstitial regions of testes of infected males at 5 days post infection (Fig. A). In addition, electron microscopy analyses showed association of virions with developing sperm within the testes as well as with mature sperm within the epididymis. Interestingly, ZIKV replication persists within the testes even after clearance from the blood. We also found high levels of viral RNA and antigen within the epididymal lumen where sperm is stored and within surrounding epithelial cells. Unexpectedly, at 21 days post infection, testes of the ZIKV-infected mice were significantly smaller, compared to those of mock-infected mice, indicating progressive testicular atrophy (Fig. B). ZIKV infection caused a reduction in serum testosterone, suggesting male fertility can be affected.

We also examine sexual transmission of ZIKV utilizing *Ifnar1*<sup>-/-</sup> mice. When ZIKV-infected male mice were mated with naïve female mice, the weight of fetuses at embryonic day 18.5 was significantly reduced compared with the control group. Additionally, we found ocular deformities in a minority of the fetuses. These results suggest that ZIKV causes fetal abnormalities after female mating with an infected male. Overall, our findings have important implications for non-vector-borne vertical transmission, as well as long-term potential reproductive deficiencies, in ZIKV-infected males.

[1] Ventura CV et al. *Lancet* **387**,228 (2016).

[2] Mansuy JM et al. *Lancet Infect Dis* **16**,1106-7 (2016).



## Mutant mRNA decay confers genetic robustness to mutations through triggering transcriptional upregulation of related genes.

Mohamed A. El-Brolosy, Andrea Rossi, Zacharias Kontarakis, Carsten Kuenne, Stefan Günther, Nana Fukuda, Carter Takacs, Shih-Lei Lai, Ryuichi Fukuda, Claudia Gerri, Khrievono Kikhi, Antonio J. Giraldez and Didier Y.R. Stainier

Max Planck Institute for Heart and Lung Research

Ludwigstrasse 43, Bad Nauheim/61231, Germany

Robustness to mutations promotes organisms' well-being and fitness. The increasing number of mutants in various model organisms showing no obvious phenotype has renewed interest into how organisms adapt to gene loss. In the presence of deleterious mutations, genetic compensation by transcriptional upregulation of related gene(s) (also known as transcriptional adaptation) has been reported in numerous systems (reviewed in [1]); however, the molecular mechanisms underlying this response remain unclear. To investigate this phenomenon, we developed and analyzed several models of transcriptional adaptation in zebrafish and mouse. We first observed that transcriptional adaptation is not caused by loss of protein function, indicating that the trigger lies upstream. We find that the increase in transcript levels is due to increased transcription, and that chromatin becomes more accessible at the upregulated genes' regulatory regions. As mutations often lead to transcripts that are degraded by the mRNA surveillance machinery, we investigated this process and found a correlation between the degree of mutant mRNA decay and the transcriptional upregulation of the related gene(s). In order to assess the role of the mutant mRNA in triggering transcriptional adaptation, we generated alleles that fail to transcribe the mutated gene and found that they do not exhibit this response. In addition, they displayed more severe phenotypes than those observed in alleles exhibiting mutant mRNA decay. Moreover, genetic inactivation of the nonsense mediated decay factor Upf1 can also lead to the loss of transcriptional adaptation. Coupling of mRNA decay and transcription has been reported previously [2]. RNA-seq analysis of wild-type and mutant cells revealed upregulation of many genes and notably an enrichment for genes sharing DNA sequence similarity with the mutated gene's coding sequence, proposing a model whereby RNA decay intermediates induce the transcriptional adaptation response. These results identify a new role for the mRNA surveillance machinery in buffering against mutations and provide insights into why some human mutations cause disease while others do not. They might also lead to the development of more effective therapies that enhance an organism's robustness to a mutation rather than correct its effect, e.g., identify novel modifier genes whose expression levels could be modulated for therapeutic purposes.

[1] El-Brolosy and Stainier, *PLOS genetics* **13**, e1006780 (2017).

[2] Haimovich et al., *Cell* **153**, 1000-1011 (2013).

## Non-coding RNAs are important regulators of adipocyte plasticity

Maude Giroud<sup>1,2,3,4</sup>, Didier F. Pisani<sup>5</sup>, Pirjo Nuutila<sup>6,7</sup>, Kirsi A. Virtanen<sup>6,8</sup>, Ez-Zoubir Amri<sup>5</sup>,  
Stephan Herzig<sup>1,2,3,4</sup> and Marcel Scheidele<sup>1,2,3,4</sup>

<sup>1</sup>Institute for Diabetes and Cancer (IDC), Helmholtz Zentrum München, German Research Center for Environmental Health, Neuherberg, Germany

<sup>2</sup>Joint Heidelberg-IDC Translational Diabetes Program, Heidelberg University Hospital, Heidelberg, Germany

<sup>3</sup>Molecular Metabolic Control, Medical Faculty, Technical University Munich, Germany

<sup>4</sup>German Center for Diabetes Research (DZD), Neuherberg, Germany

<sup>5</sup>Univ. Nice Sophia Antipolis, CNRS, Inserm, iBV, Nice, France

<sup>6</sup>Endocrinology, Turku University Hospital, Turku, Finland

<sup>7</sup>Turku University Hospital, Turku, Finland

<sup>8</sup>Turku PET Centre, University of Turku, Turku, Finland

In response to cold exposure or  $\beta$ 3-adrenoceptor stimulation, brown adipose tissue (BAT) is able to combust energy to form heat, a phenomenon known as non-shivering thermogenesis. In this context, energy-storing white adipocytes can be converted into thermogenic adipocytes, also called “inducible brown”, “brite” or “beige” adipocytes.

In humans, thermogenic adipocytes were long thought to be exclusively present in the interscapular and perirenal area of newborns. Nevertheless, around nine years ago, the discovery of thermogenic brown-like adipocytes found within human white adipose tissue (WAT) has opened a novel avenue to combat overweight/obesity and associated diseases.

The vast majority of our genome is non-coding but nevertheless active, meaning non-coding RNAs (ncRNAs) are transcribed. Regulatory ncRNAs can be divided into two categories: the small ncRNAs (sncRNAs), including microRNAs, and the long ncRNAs (lncRNAs).

In this presentation I will first focus on the role of two microRNAs in adipose tissue plasticity. Based on molecular and functional studies we have characterized let-7i-5p [1] and miR-125b-5p [2] as important candidates involved in the formation of brite adipocytes in human cells and mouse adipose tissues. Second, I will present a study where we applied a whole human genome comparative transcriptomics approach and identified lncRNA AATBC to be highly enriched in BAT compared to WAT, implicating a potential role in thermogenesis. AATBC loss-of-function studies in human cells affect the acquisition of the thermogenic phenotype marked by a decreased expression of several brown marker genes, thermogenic function and mitochondrial DNA content.

Overall, these data provide evidence that ncRNAs have an important impact on adipocyte plasticity and add an additional regulatory layer to the transcriptional network.

[1] M.Giroud *et al.*, Sci. Rep. 6, 28613 (2016).

[2] M.Giroud *et al.*, Mol. Metab. 5, 615–625 (2016).

This work was kindly supported by the European FP7 project DIABAT, the German Center for Diabetes Research (DZD) and the Alexander von Humboldt foundation.

## A novel role for chromatin dynamics in maintaining genome stability

Rachel Bayley<sup>1</sup>, Koichi Sato<sup>2</sup>, Grant Stewart<sup>1</sup>, Martin R Higgs<sup>1</sup>

1) Institute of Cancer and Genomic Sciences, University of Birmingham, Birmingham, B15 2TT, UK

2) Department of Electrical Engineering and Bioscience, Waseda University, Shinjuku, Tokyo 169-12, 8050, Japan

Normal cellular processes such as DNA replication and transcription require dynamic changes in chromatin structure. One important part of this is histone mobility, which includes the removal of histones from parental DNA and the placement of new histones onto newly synthesised DNA. These events are regulated by a number of canonical histone chaperones such as CAF-1, HIRA and FACT [1]. In addition, the presence of post-translational modifications (PTMs) including methylation and acetylation regulate essential cellular processes through their distinct functions [2]. Although a considerable amount is known regarding histone mobility during cellular homeostasis, there has been little study of such events during perturbed replication, a state known as replication stress. If unresolved, replication stress can cause genome instability which has been linked to the development of cancer [3].

Here, we show that the histone H3-modifying enzyme SETD1A plays a novel role in maintaining genome stability in response to replication stress, through its ability to catalyse the methylation of lysine4 of histone H3 (H3K4) and influence histone chaperoning. Human cells depleted of SETD1A by transient siRNA knock down display increased sensitivity to replication stress induced by mitomycin C, characterised by the increased degradation of newly synthesised DNA. Mechanistically, we observe that SETD1A catalyses the methylation of H3K4 at replication forks, which enhances histone mobility. Preventing H3K4 methylation or abrogating histone chaperone activity induces the degradation of replicated DNA.

This work identifies that histone dynamics play an important role in protecting newly replicated DNA from attack, and that histone PTMs are vital for this protection. We also describe a novel role for SETD1A as a DNA damage response specific histone-modifying enzyme required for the activity of histone chaperone proteins in order to maintain genome stability. Since such genomic integrity is vital to prevent cellular transformation and cancer, this work sheds new light on the dynamics of histones in preventing disease.

[1] CM Hammond, CB Strømme, H Huang, DJ Patel and A Groth, Nature Reviews Molecular Cell Biology, 18,141–158 (2017).

[2] AJ Bannister and T Kouzarides, Cell Research, 21(3): 381–395, (2011).

[3] MK Zeman and KA Cimprich, Nature Cell Biology, 16(1):2-9, (2014).



## Exome sequencing in human bladder exstrophy and knockdown studies in zebrafish implicate *SLC20A1* as candidate gene and major regulator of urinary tract development

J.M. Schmidt<sup>1,2</sup>, Ö. Yilmaz<sup>2</sup>, R. Zhang<sup>1</sup>, A.S. Japp<sup>3</sup>, M. Pleschka<sup>1,2</sup>, H. Reutter<sup>1,4</sup>, B. Odermatt<sup>2</sup>

<sup>1</sup>Institute of Human Genetics, <sup>2</sup>Institute of Anatomy, <sup>3</sup>Institute of Neuropathology,

<sup>4</sup>Department of Neonatology and Pediatric Intensive Care, University of Bonn, University Hospital Bonn, School of Medicine, Bonn, Germany

**Introduction:** Exome sequencing in patients with bladder exstrophy-epispadias complex (BEEC) identified one novel *de novo* variant (p.G237R) in *SLC20A1* in a patient with cloacal exstrophy. Re-sequencing of 526 BEEC patients identified one additional novel *de novo* variant (p.V298A) and one novel maternally transmitted variant (p.K441Q) from an affected mother to her affected son. All three variants were predicted to be disease causing. The BEEC represents the severe end of human congenital anomalies of the kidney and urinary tract (CAKUT). To follow up on our genetic findings we investigated the developmental function of *slc20a1a* in developing zebrafish larvae (zfl) performing Morpholino (MO) knockdown (KD) experiments.

The urinary tract in zfl consists of two fused glomeruli and their corresponding pronephric ducts. The segmentation of the pronephros is similar to human nephrons. There is no urinary bladder described in zf, but the terminal parts of the collecting ducts, as most distal part of the pronephros, fuse and build a caudal opening at the cloaca of zfl. *SLC20A1* encodes for a Na<sup>+</sup>/PO<sub>4</sub> co-transporter known to play a role in proliferation and TNF-induced apoptosis. It is ubiquously expressed in mammals. Its zf orthologue *slc20a1a* is frequently used as a pronephric in situ hybridization (ISH) marker.

**Methods:** *Slc20a1a* KD in zfl was done by injecting antisense oligonucleotides with a morpholino<sup>®</sup> backbone into 1-4 cell staged eggs, blocking the gene's translation. Specificity of the MO was shown by Western Blot and rescue experiments, co-injecting human mRNA transcripts of *SLC20A1*. We characterized the MO phenotypes using different assays such as sulforhodamine 101 excretion, ISH with several urogenital marker probes, immunohistochemistry (IHC) staining and the transgenic zf reporter line *Tg(wt1b:GFP)*. IHC was performed on paraffin sections using proliferation and apoptosis markers.

**Results:** MO KD of *Slc20a1a* in zfl results in a severe lethal phenotype that affects development of different organ systems. We see a grading of lethality and severity of the phenotypes depending on the strength of KD, identifying *slc20a1a* as a major regulator of zf development. Focusing on urinary tract, we see formation of pronephric cysts and disorganization of the cloaca. Sulforhodamine 101 assay uncovers that there are severe opening defects of the cloaca for the intestine in KD zfl. IHC shows defects in proliferation and apoptosis compared to control zfl.

**Discussion:** Our data suggests *slc20a1a* as a major player in zf development. Mild MO phenotypes present with urinary tract anomalies such as pronephric cysts and disorganization of the cloaca. Severe MO phenotypes present with hydrocephalus, vertebral defects, disorganization of the eyes and cardiovascular anomalies with a high lethality among zfl, underlining the overall importance of *slc20a1a* during embryonic development. In conclusion, exome sequencing in human bladder exstrophy and developmental biology studies in zfl implicate *SLC20A1* as a disease gene for human BEEC and as a major regulator of urinary tract development.

## Transcriptome adaptation to cell shape

Scott Berry, Lucas Pelkmans

Institute of Molecular Life Sciences, University of Zurich  
Winterthurerstrasse 190, CH-8057 Zurich, Switzerland

Gene expression can be highly heterogeneous within tissues and in cell populations, with genetically-identical cells displaying widely different numbers of transcripts for the same genes. Although often referred to as gene expression ‘noise’, a large part of this heterogeneity can be explained by cell size variation, with larger cells generally having a greater number of transcripts [1]. Such ‘scaling’ of gene expression with cell size is not the only factor contributing to heterogeneity, however. Quantitative analysis of transcript abundance suggests that transcriptomes of cells are precisely adapted to the protein content, surface area, cell cycle stage and population context of each cell [2]. The mechanistic basis of such ‘single-cell’ gene regulation remains largely unexplored.

Here we investigate the class of human genes whose transcript abundance shows particularly strong correlation with cell surface area, rather than cell volume. This class is enriched for genes encoding proteins related to membrane function, suggesting that single cells regulate these genes according to membrane abundance – to eventually ensure optimal densities of membrane-associated proteins. Using single-molecule FISH experiments, we find that the production rate rather than the degradation rate of these transcripts is coordinated with membrane area. Moreover, we find that the abundance of these transcripts can be directly reduced in proportion to cell surface area by constraining cells using two-dimensional micropatterns (Figure 1). Together, these two observations show that human cells are actively sensing their surface area and transmitting this information to the nucleus to regulate the transcription of a subset of genes.

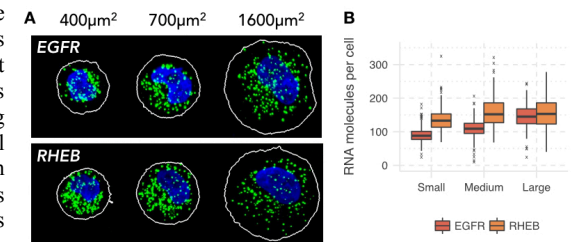


**Figure 1:** Expression of area-scaling genes such as epidermal growth-factor receptor (*EGFR*) can be directly modulated by restricting the availability of growth surface. In contrast, volume-scaling genes such as Ras-homolog enriched in brain (*RHEB*) show limited response. (A) Single-molecule FISH (green) shows RNA transcripts of *EGFR* and *RHEB*. DNA (blue) and cell outlines (white). (B) Quantification of transcripts per cell across hundreds of single cells per condition.

- [1] O. Padovan-Merhar, et al., Mol. Cell **58** 339–352 (2015).
- [2] N. Battich, T. Stoeger, L. Pelkmans, Cell **163**, 1596–1610 (2015).

## Pore Architecture and Gating Mechanism of TRIC Channels

Hanting Yang<sup>1,2#</sup>, **Miaohui Hu**<sup>1,2#</sup>, Jianli Guo<sup>1</sup>, Xiaomin Ou<sup>1</sup>, and Zhenfeng Liu<sup>1\*</sup>

<sup>1</sup>National Laboratory of Biomacromolecules, CAS Center for Excellence in Biomacromolecules, Institute of Biophysics, Chinese Academy of Sciences, Beijing 100101, China.

<sup>2</sup>University of Chinese Academy of Sciences, Beijing 100049, China.

# These authors contributed equally to the work.

\* Corresponding author.

Trimeric Intracellular Cation (TRIC) channels are a family of monovalent cation channels permeable to  $K^+$  and  $Na^+$ , and is essential for supporting the release of  $Ca^{2+}$  from sarcoplasmic reticulum (SR) or endoplasmic reticulum (ER) into the cytoplasm. Two subtypes of TRIC channels, namely TRIC-A and B, have been identified and their dysfunction would cause disorders of skeletal and cardiac muscle contraction, blood pressure regulation, lung development and bone formation. Despite that the functions of TRIC channels have been studied extensively, little is known about their architecture or gating mechanism.

Here we present the structures of TRIC-B channels from *Caenorhabditis elegans* (CeTRIC-B1 and CeTRIC-B2) in complex with endogenous phosphatidylinositol 4,5-bisphosphate (PIP<sub>2</sub>) molecules. The CeTRIC-B proteins and PIP<sub>2</sub> molecules assemble into a symmetrical homotrimeric complex. Each monomer contains an hourglass-shaped hydrophilic pore harbored within a seven-transmembrane-helix domain. The three monomers may cooperate with each other when they open their internal pores to permeate monovalent cations. Buried inside the cytoplasmic vestibule, the negatively-charged head group of PIP<sub>2</sub> binds specifically to two highly conserved basic amino acid residues on the pore lumen surface, and thus contributes to the formation of pore and gating process. Meanwhile, the hydrophobic tails of PIP<sub>2</sub> mediate trimerization of TRIC channels.

Structure and functional data suggest that calcium ions may stimulate the channels activity by modulating the conformation of a cytoplasmic loop between M5 and M6.

Upon binding of  $Ca^{2+}$ , a dramatic conformation change occurs in the loop region on the cytoplasmic side between the 5th and the 6th transmembrane helix (M5-6 loop). The M5-6 loop in CeTRIC-B2 is distant from the monomeric pore, while the corresponding part in CeTRIC-B1 is close to the pore and shorter in length. The movement of M5-6 loop directly changes the surface electrostatic potential distribution at the entrance of the cytoplasmic side of the monomeric pore. Through structural analysis and functional assays, we have proposed a mechanistic model to account for the gating process of TRIC channels stimulated by cytoplasmic  $Ca^{2+}$  and the application of transmembrane voltage.

In summary, our studies revealed the three-dimensional structures of the TRIC channels and provide mechanistic insights into their pivotal functions in the regulation of intracellular  $Ca^{2+}$  signaling process.

## Morphologically mapping the development of the blood-brain barrier using high resolution electron microscopy

Shireen Mentor, David Fisher

Neurobiology Group, Department of Medical Biosciences, Faculty of Natural Sciences, University of the Western Cape, Robert Sobukwe Road, Bellville, Cape Town, 7535, South Africa

The morphological profiling of the brain endothelial cell (BEC) with its concomitant structures presents a novel description on blood-brain barrier (BBB) development. Brain capillaries forms the anatomical basis of the BBB and constitutes the primary regulatory interface for the passage of blood-borne substances into the central nervous system (CNS). Brain capillaries differ from other systemic capillaries in that their paracellular pathways are virtually impermeable, relegating transport to transcellular routes. The BBB elicits its homeostatic effects through the presence of intercellular tight junction (TJ) proteins, forming wide rows of overlapping occlusions that prevent the leakage of blood-borne substances. TJs consist of occludin, junctional adhesion molecules, claudins, and zonula occludens which regulate the lateral diffusion between the apical and basolateral membranes of BECs, re-enforcing its “gate-like” function within the paracellular pathway [1]. Previously, imaging the brain capillaries was fraught with technical difficulty. We hereby propose a novel experimental design to visualize the molecular architecture of capillary endothelium. We employed high resolution scanning electron microscopy (HRSEM), in order to map morphologically the orientation, interaction and proliferation of the BECs, and for the first time, visualize on a nano-scale the cell-to-cell interaction underpinning the development of the BBB. We qualitatively analyzed how these ultrastructures facilitate *in vitro* BBB construction. The HRSEM micrographs depict the formation of specialized nano-tubular structures which are aligned and synchronized to bring about cell membrane continuity. Cell-to-cell communication using exosome formation, specifically on the apico-lateral membrane between adjacent BECs, is fundamental in directing the engagement between the nano-tubules within the paracellular space. We have identified several types of nano-tubules, some of which have their distal ends fused to the membrane of the adjacent cell, tunneling nano-tubules (TUNTs), allowing for the direct transfer of substances to a distinct apico-lateral location. Other nano-tubules, ‘rope-like’ tethering nano-tubules (TENTs), tether themselves to adjacent cells allowing for the physical pulling of the cellular membrane across the paracellular space. The latter mechanism is mirrored by the juxtapositioned adjacent cell’s membrane, thus allowing for both adjacent cell membranes to be brought into contact, which is crucial for TJ contact. Yet the attachment of TJs does not appear to bring about a tight paracellular seal. Further tethering activity, by pulling sections of plasma membrane over the TJ contacts, seals off the paracellular space. This study reports for the first time on: 1) the apico-lateral establishment of topographical ultrastructures (TENTs and TUNTs) involved in BBB formation, 2) we propose a role for the exosomes in the formation of both TUNTs and TENTs, and 3) we present evidence for the sequential formation of the BBB by presenting a mechanism for the juxtaposing hemifusion of BEC apico-lateral membranes as a precedent event to BBB paracellular impermeability. The study provides key insights into the BBB’s development and structure, which will allow clinicians and neurologists to re-strategize novel methodologies to manipulate the entry of drugs into the brain.

[1] I.A. Krizbai, Acta Neurobiol Exp **71**, 113-128, (2011).

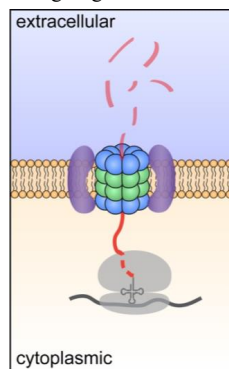
## Coupled protein synthesis and degradation through a neuronal 20S plasma membrane proteasome complex

*Kapil V. Ramachandran, Jack M. Fu, Thomas Schaffer, Seth S. Margolis*

Department of Cell Biology, Harvard Medical School  
240 Longwood Avenue, Boston, MA 02115

In the nervous system, rapidly occurring processes such as neuronal transmission and calcium signaling are affected by short-term inhibition of proteasome function. It is unclear how proteasomes are able to acutely regulate such processes, as this action is inconsistent with their canonical role in proteostasis. We discovered a mammalian nervous-system-specific membrane 20S plasma proteasome complex that directly and rapidly modulates neuronal function by degrading intracellular proteins into extracellular peptides that can stimulate neuronal signaling<sup>1</sup>. This proteasome complex is closely associated with neuronal plasma membranes, exposed to the extracellular space, and catalytically active. Selective inhibition of the membrane proteasome complex by a cell-impermeable proteasome inhibitor blocked the production of extracellular peptides and attenuated neuronal-activity-induced calcium signaling. Moreover, we observed that membrane-proteasome-derived peptides were sufficient to induce calcium signaling.

Analyzing the composition of the neuronal plasma membrane proteasome (NMP), we did not find canonical ubiquitin-proteasome components required for recognizing a ubiquitinated protein. This raised the fundamental question of how substrates were being targeted to the NMP for degradation into extracellular peptides. Remarkably, we observed newly synthesized polypeptides were rapidly turned over by the NMP in a stimulation-dependent manner. Using parameters determined in these experiments, we constructed Markov process chain models in silico which predicted that the kinetics of this process necessitate coordination of translation and degradation. In a series of biochemical analyses, this predicted coordination was instantiated by NMP-mediated and ubiquitin-independent degradation of ribosome-associated nascent polypeptides. This coordination is enabled by the direct activity- and nascent chain-dependent association of ribosomes with the NMP. Using in-depth, global, and unbiased mass spectrometry, we identified the nascent protein substrates of the NMP. Among these substrates, we found that immediate-early gene products c-Fos and Npas4 are targeted by the NMP during ongoing activity-dependent protein synthesis, prior to activity-induced transcriptional responses. Together, these findings generally define a neuronal-specific ubiquitin-independent protein quality control program, specified as coupled protein synthesis and degradation through 20S neuronal plasma membrane proteasomes.



[1] **Kapil V. Ramachandran & Seth S. Margolis.** A mammalian nervous-system-specific plasma membrane proteasome complex that modulates neuronal function. *Nature Structural and Molecular Biology*. 2017; 24, 419–430

## Pulsing and propagating features of ERK MAPK signal in skin.

*Toru Hiratsuka<sup>1</sup>, Ignacio Bordeu<sup>2</sup>, Fiona M. Watt<sup>1</sup>*

1. King's College London, Centre for Stem Cells and Regenerative Medicine, 28th Floor, Tower Wing, Guy's Hospital Campus, Great Maze Pond, London SE1 9RT, UK
2. Department of Mathematics, Imperial College London, 180 Queen's Gate, London SW7 2BZ, UK.

ERK MAPK pathway regulates multiple cellular events such as cell proliferation, migration, and differentiation. Mammalian tissue is an ensemble of heterogeneous cells that originates from stem cells and replenished by their proliferation and differentiation. How the same kinase determines the cell fates, however, has yet to be elucidated.

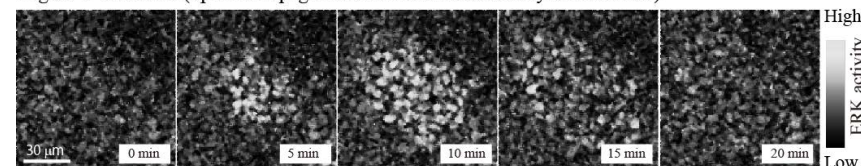
Here we time-lapse monitored ERK MAPK dynamics in living mouse skin and human keratinocytes with single cell resolution. Interestingly, the physiological ERK MAPK activity was not simply stable and unchanged but dynamically changed with pulse activations and propagations.

In mouse epidermis, ERK activity showed occasional bursts and propagation to neighboring cells, which we named SPREAD (spatial propagation of ERK activity distribution) (Figure 1). The event was significantly associated with keratinocyte proliferation. Furthermore, the observation of epithelial wound healing revealed ERK activity repetitively propagated from the wound edge, which was associated with collective cell migration [1].

In human epidermal stem cells, ERK activity time-series dynamically changed with modulations in pulse activations during transition of stem cell states from quiescence to proliferation, and to differentiation.

These results provide a fresh insight into how intracellular signal is dynamically regulated and communicate with surrounding cells for tissue homeostasis and regeneration.

Figure 1. SPREAD (Spatial Propagation of Radial ERK Activity Distribution)



[1] Hiratsuka T, Fujita Y, Naoki H, Aoki K, Kamioka Y, Matsuda M. Intercellular propagation of extracellular signal-regulated kinase activation revealed by in vivo imaging of mouse skin. *Elife* 4: e05178 (2015).

## Dissecting the Contribution of Recurrent p53 Gain-of-Function Mutations to Pancreatic Tumorigenesis

Paffenholz SV<sup>1\*</sup>, Sánchez-Rivera FJ<sup>1\*</sup>, Leibold J<sup>1</sup>, Kastenhuber ER<sup>1</sup>, Lowe SW<sup>1</sup>

<sup>1</sup> Department of Cancer Biology and Genetics, Memorial Sloan Kettering Cancer Center, New York, NY 10065, USA.

\* These authors contributed equally to this work.

70 % of patients with pancreatic ductal adenocarcinoma (PDAC), a lethal disease with dismal prognosis, harbor *TP53* mutations [1]. The p53 tumor suppressor acts as a transcription factor that promotes apoptosis, senescence and differentiation [2]. Despite the fact that inactivation of p53 function contributes to tumorigenesis, the majority of cancer-associated alterations in the *TP53* gene are missense mutations. Recent evidence suggests that some of those alleles endow p53 with gain-of-function (GOF) activities, indicating that not all p53 mutations are functionally redundant [3]. To date, this large degree of functional heterogeneity within the spectrum of p53 mutations has not been addressed by systematic studies.

Here we describe a novel CRISPR-Cas9 Base Editing-based (BE) approach to rapidly and accurately model *TP53* C>T (or G>A) missense mutations in a cutting- and template-independent manner [4]. We developed a bioinformatic pipeline that can use any mutation file as input (e.g. TCGA datasets) and subsequently determine the recurrence of mutations in tumor-associated genes and the sgRNA sequence required to model it using BE. The analysis identified more than 60 recurrent and engineerable mutations in *TP53*, which include hotspot mutations with known GOF activity, e.g. R273C. We established a platform to engineer and interrogate the R270C mutation in mice (corresponds to R273C in humans) *in vivo* using direct pancreas electroporation. Novel transposon vectors allow for Kras<sup>G12D</sup>-dependent pancreatic tumor initiation coupled to BE of endogenous Trp53 and temporal manipulation of p53 expression using a Doxycycline-inducible shRNA. Pancreatic tumors harboring the desired p53 mutation were observed in a time frame of 40 days. shRNA-mediated depletion of the p53<sup>R273C</sup> mutant protein in established tumors led to substantial tumor regression (Fig. 1). This demonstrates – for the first time – that the R270C mutation has potent GOF activity in pancreatic tumors and its continuous expression is required for tumor maintenance *in vivo*. We envision that the described platform can be applied to systematically interrogate the top recurrent and engineerable p53 mutants *in vivo* and to dissect molecular mechanisms underlying the biology of these novel p53 mutant alleles.

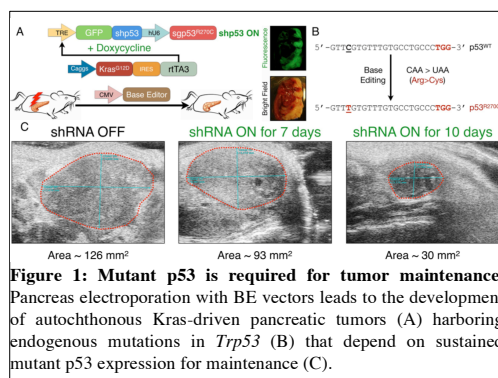


**Figure 1: Mutant p53 is required for tumor maintenance.** Pancreas electroporation with BE vectors leads to the development of autochthonous Kras-driven pancreatic tumors (A) harboring endogenous mutations in *Trp53* (B) that depend on sustained mutant p53 expression for maintenance (C).

## In vivo, label-free evaluation of mitochondrial dynamics in human skin enables non-invasive classification of malignant skin lesions.

Dimitra Pouli<sup>1</sup>, Mihaela Balu<sup>2</sup>, Carlo A. Alonzo<sup>1</sup>, Zhiyi Liu<sup>1</sup>, Kyle P. Quinn<sup>1\*</sup>, Francisca Rius-Diaz<sup>3</sup>, Ronald M. Harris<sup>4</sup>, Kristen M. Kelly<sup>4</sup>, Bruce J. Tromberg<sup>2</sup>, Irene Georgakoudi<sup>1</sup>

<sup>1</sup> Department of Biomedical Engineering, Tufts University, 4 Colby Street, Medford, MA 02155

<sup>2</sup> Laser Microbeam and Medical Program, Beckman Laser Institute, University of California, Irvine, CA, 1002 Health Sciences Rd., Irvine, USA 92612

<sup>3</sup> Health Public Department, Faculty of Medicine, University of Malaga, 32 Louis Pasteur Boulevard, 29071 Málaga, Spain

<sup>4</sup> Department of Dermatology, University of California–Irvine, 1 Medical Plaza Dr, Irvine, CA 92697

\* Department of Biomedical Engineering, University of Arkansas, 120 John A. White, Jr. Engineering Hall, Fayetteville, AR 72701

The dynamic nature of mitochondrial function and organization and its implications in the pathophysiology of a variety of human diseases are being increasingly recognized in recent years. As mitochondria are key participating organelles in cellular homeostasis, techniques that allow monitoring of their function can prove invaluable in extracting diagnostic biomarkers or monitoring response to novel treatments. Unfortunately, established methods to assess mitochondrial structural organization rely on the use of exogenous contrast and are typically limited in the characterization of two-dimensional samples. In this study, we establish that we can evaluate mitochondrial organization non-invasively, *in vivo*, in three-dimensional human tissues through endogenous two-photon excited fluorescence (TPEF) images. To establish and demonstrate the translational potential of spatial mitochondrial organization as a diagnostic biomarker, we analyze three dimensional image stacks from healthy and diseased human skin using a multiphoton clinical tomograph (JenLab). Specifically, to evaluate our analytical technique in a broad spectrum of clinical needs, we incorporate in our study tissue data acquired from a variety of skin cancers, including basal cell carcinomas, invasive and in situ melanomas, as well as a small sample of tissues where only inflammation is present in the dermis. We discover that the healthy epidermis presents with depth dependent organization trends that correlate highly with its stratification continuum. On the contrary, the morphofunctional depth-dependent patterns become abolished in diseased tissues and these quantitative differences are exploited for automated, predictive tissue classification with high sensitivity and specificity. Given the importance of mitochondrial dynamics not only in cancer development, but also in a number of diseases such as diabetes and neurodegenerative disorders, the method described in our study could serve as an important diagnostic and/or treatment monitoring tool for a broad range of significant biomedical applications.

- [1] S Jones, X Zhang, ..., B Vogelstein, VE Velculescu, and KW Kinzler, "Core signaling pathways in human pancreatic cancers revealed by global genomic analyses.," *Science*, vol. 321, no. 5897, pp. 1801–1806, Sep. 2008.
- [2] D Lane and A Levine, "p53 Research: the past thirty years and the next thirty years.," *Cold Spring Harbor Perspectives in Biology*, vol. 2, no. 12, pp. a000893–a000893, Dec. 2010.
- [3] WA Freed-Pastor and C Prives, "Mutant p53: one name, many proteins.," *Genes Dev.*, vol. 26, no. 12, pp. 1268–1286, Jun. 2012.
- [4] AC Komor, YB Kim, MS Packer, JA Zuris, and DR Liu, "Programmable editing of a target base in genomic DNA without double-stranded DNA cleavage.," *Nature*, vol. 533, no. 7603, pp. 1–17, Apr. 2016.



## AIM2 activation causes intestinal toxicity in chemotherapy

Qiaoshi Lian<sup>1,4,\*</sup>, Jun Xu<sup>2,4,\*</sup>, Shanshan Yan<sup>1,5,\*</sup>, Min Huang<sup>2,\*</sup>, Honghua Ding<sup>6</sup>, Xiaoyu Sun<sup>3</sup>, Aiwei Bi<sup>2</sup>, Jian Ding<sup>2</sup>, Bing Sun<sup>1,3</sup>, Meiyu Geng<sup>2</sup>

<sup>1</sup>State Key Laboratory of Cell Biology, CAS Center for Excellence in Molecular Cell Science, Shanghai Institute of Biochemistry and Cell Biology, Chinese Academy of Sciences, 320 Yueyang Road, Shanghai 200031, China; <sup>2</sup>Division of Antitumor Pharmacology, State Key Laboratory of Drug Research, Shanghai Institute of Materia Medica, Chinese Academy of Sciences, Shanghai 201203, China; <sup>3</sup>CAS Key Laboratory of Molecular Virology & Immunology, Institute Pasteur of Shanghai, Chinese Academy of Sciences, 320 Yueyang Road, Shanghai 200031, China; <sup>4</sup>University of Chinese Academy of Sciences, Beijing 100049, China; <sup>5</sup>School of Life Sciences, University of Science and Technology of China, Hefei 230022, China; <sup>6</sup>Department of Oncology, Shanghai General Hospital, Shanghai Jiao Tong University School of Medicine, Shanghai 200080, China.

Chemotherapies are known often to induce severe gastrointestinal tract toxicity but the underlying mechanism remains unclear. This study considers the widely applied cytotoxic agent irinotecan (CPT-11) as a representative agent and demonstrates that treatment induces massive release of double-strand DNA from the intestine that accounts for the dose-limiting intestinal toxicity of the compound. Specifically, “self-DNA” released through exosome secretion enters the cytosol of innate immune cells and activates the AIM2 (absent in melanoma 2) inflammasome. This leads to mature IL-1 $\beta$  and IL-18 secretion and induces intestinal mucositis and late-onset diarrhoea. Interestingly, abrogation of AIM2 signalling, either in AIM2-deficient mice or by a pharmacological inhibitor such as thalidomide, significantly reduces the incidence of drug-induced diarrhoea without affecting the anticancer efficacy of CPT-11. These findings provide mechanistic insights into how chemotherapy triggers innate immune responses causing intestinal toxicity, and reveal new chemotherapy regimens that maintain anti-tumour effects but circumvent the associated adverse inflammatory response.



**Figure 1. The War of Chemotherapy.** The cover is designed based on the film ‘Star Wars’. IEC (Flamed Star) is attacked by chemotherapeutic drugs (Capsule-like Bombs), then dsDNA (Black Knight) escapes from IEC to innate immune cell (Blue Star) via exosome (Spaceship) delivery. Finally, dsDNA triggers AIM2 inflammasome activation, leading to the inflammation-mediated IECs damage (Cell Wars).

## Inhalable nanoparticles for *in vivo* genome editing mediated by crispr-cas9 delivery for undruggable *KRAS* driven lung cancers

Aditi Mehta<sup>1</sup>, Georgios Stathopoulos<sup>2</sup>, Olivia Merkel<sup>1</sup>

<sup>1</sup> Department of Pharmacy, Ludwig-Maximilians-University of Munich. <sup>2</sup> Institut für Lungenbiologie, Comprehensive Pneumology Center, Helmholtz Zentrum München

*KRAS* is the most frequently mutated gene in human cancers, with most mutations occurring in codon 12 or 13. Despite its direct involvement in malignancy and intensive effort, no effective pharmacological inhibitor of *KRAS* has been developed. Due to its important role in cell signalling, picomolar affinity between *KRAS* and GTP, and the relatively smooth protein surface, *KRAS* has proved to be an impossible target for novel small molecule drugs, and *KRAS* tumours are often regarded untreatable.

In comparison to systemic chemotherapeutic anti-cancer drugs, the direct localized administration of nucleic acids via the pulmonary route allows higher retention in lung tissues and reduces systemic toxicity for better treatments of lung cancer. Using the efficient and precise CRISPR-Cas9 gene editing approach, mutant *KRAS* alleles can be deleted or specific mutations can be corrected resulting in sudden cessation of signalling and ultimate cell death. Inhibition of an initiating oncogene often leads to extensive tumour cell death, a phenomenon known as oncogene addiction. For achieving targeted delivery of the pDNA to lung cancer cells, we used affibodies against ERBB3, another member of the EGFR Receptor Tyrosine Kinase family. We found high levels of ERBB3 on the surface of lung cancer cell lines and *Kras* mutant tumour models.

Lung cancer cell lines known to carry *Kras* mutations (AE-17, A549, A427 etc) were specifically transfected with the Cas9-sgRNA specific to the mutant allele, thereby deleting it. Subsequently, hallmarks of cancer cells, such as cell survival, proliferation, migration and anchorage independent growth were evaluated. The therapeutic potential of this study was evaluated *in vivo* using an orthotopic mouse model and the nanoparticle-plasmid complex was injected into the pleural space of tumor bearing mice.

This project aims to address three major obstacles: 1. The ‘undruggable’ nature of *KRAS* driven lung cancers; 2. Efficient and safe pulmonary delivery of nucleic acids to target cells; 3. The dosage and administration of nucleic acids delivered to target cells, thereby modulating the duration and magnitude of nuclease expression controlling on-and off-target effects.

## Microengineering Approaches to Red Blood Cell-Based Diagnostics and Drug Delivery

Yunus Alapan<sup>1</sup>, Jane A. Little<sup>2</sup>, Umut A. Gurkan<sup>2</sup>, Metin Sitti<sup>1</sup>

<sup>1</sup>Max Planck Institute for Intelligent Systems  
Heisenbergstraße 3, Stuttgart/70569, Germany

<sup>2</sup>Case Western Reserve University  
10900 Euclid Avenue, Cleveland, OH/44106, USA

Red blood cells (RBCs) are specialized carriers with high surface-to-volume ratio, deformability, and minimal interaction with blood vessels. Due to their centrality in human physiology, RBCs hold crucial information on pathophysiology of several diseases, including hemoglobinopathies, such as sickle cell disease (SCD) [1]. In addition, RBCs have attracted great interest as non-genetically engineered carriers of imaging agents and drugs for targeted therapies. We have developed three key microengineered platforms that can probe or manipulate RBCs: (1) micro-electrophoresis chip for low-cost and rapid diagnosis of hemoglobinopathies, (2) microfluidic RBC adhesion assay for point-of-care monitoring sickle cell disease patients, and (3) biohybrid RBC microswimmers for targeted drug delivery.

SCD is a genetically inherited debilitating illness that requires early diagnosis after birth and constant monitoring throughout the life span of the patient. To address this unmet clinical need, we developed the HemeChip technology, which can separate hemoglobin types, based on their net charge, in a finger-prick volume of blood on a piece of paper that is housed in a micro-engineered chip [2]. HemeChip offers a low-cost (<1\$), rapid (<10 min), accurate (<90% sensitivity and specificity), and fully portable platform for diagnosis of SCD.

Monitoring of SCD patients presents insurmountable challenges due to heterogeneities among patients, as well as in the same individual over time. To overcome this clinical barrier, we developed a clinically applicable microfluidic assay (SCD Biochip) mimicking microvasculature environment for rapid, preprocessing free, and standardized interrogation of RBC adhesion in whole blood [3]. RBC adhesion measured in the microfluidic device from more than 100 subject blood samples showed strong associations with clinical phenotypes, including hemolysis and reticulocytosis; and longitudinal quantitative RBC adhesion measurements successfully tracked physiological changes in patients over time.

RBCs have received significant attention as a model carrier due to their biocompatibility and deformability compared to conventional synthetic carriers. Despite such advantages, RBCs have been mainly utilized as passive carriers. To transform RBCs from passive carriers into active and guidable cargo carriers towards targeted drug delivery, we developed a biohybrid microswimmer composed of bioengineered motile bacteria and RBCs loaded with a model anti-cancer drug and superparamagnetic iron oxide nanoparticles [4]. RBC microswimmers are propelled autonomously, can be magnetically steered, and terminated via a near infrared triggered hyperthermia termination switch. RBC microswimmers demonstrate integration of the nature's one of the most efficient swimmers (bacterium) and carriers (RBC) to create the blueprint for the next generation of multimodal, targeted cargo delivery systems.

- [1] Y. Alapan, A. Fraiwan, *et al.*, Expert Review of Medical Devices, 13, 1073-1093, (2016)
- [2] R. Ung, Y. Alapan, *et al.*, Blood, 126, 3379-3379, (2015)
- [3] Y. Alapan, C. Kim, *et al.*, Translational Research, 173, 74-91, (2016)
- [4] Y. Alapan, O. Yasa, *et al.*, Science Robotics, in press, (2018)

## Dynamic MRI as outcome predictor for Lung Volume Reduction Surgery in patients with severe emphysema

Martini K, Caviezel C, Schneider D, Milanese G, Schmitt-Opitz I, Weder W, Frauenfelder T

Institute for Diagnostic and Interventional Radiology, University Hospital Zurich,  
Rämistrasse 100, 8091 Zürich, Switzerland

**Objective:** Lung volume reduction surgery (LVRS) improves lung function, dyspnea and even survival in carefully selected emphysema patients. Despite rigorous and well-accepted inclusion criteria, the pre-operative prediction of responders is still an issue. We hypothesize a significant correlation between parameters of pre-operative dynamic MRI (dMRI) and postoperative outcome, measured by pulmonary function tests (PFT).

**Material and Methods:** In this prospective clinical trial, dMRI was performed on a 3T-MRI-scanner obtaining dynamic sequences of the lung during two breath-cycles for both lungs the day before and 3 months after surgery, herein termed as pre- and post-LVRS MRI. Quantitative measurements were performed on sagittal planes for the left and right lung in pre- and post LVRS MRI at fully inspiration and expiration (**Figure 1**): lung height (from lung apex to dome of hemidiaphragm), anteroposterior (AP) diameter (through hilum at widest point), hemidiaphragm height and area (from apex of hemidiaphragm to line connecting anterior and posterior costophrenic angles) as well as lung area and perimeter. Additionally dynamic changes in hemidiaphragmatic area and height for one breath cycle were measured. Measured parameters were normalized by division through patient-height. Additionally, all patients underwent PFT pre- and post-LVRS. The cut-off value for treatment-benefit after LVRS was defined as a 30% increase of forced expiratory volume in one second (FEV1%).

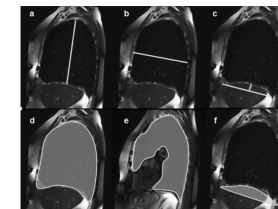


Figure 1: Lung measurements

**Results:** Thirty-nine consecutive patients (15 females, median age 61 years) with all types of emphysema morphology underwent LVRS and were included in the study. On expiration mean lung area on both sides ( $p_{\text{right}}=0.001$  and  $p_{\text{left}}=0.016$ ) as well as AP-diameter for the right lung ( $p_{\text{right}}=0.003$ ) improved significantly in patients undergoing LVRS. Dynamic measurements showed significant differences pre- and post LVRS on the right lung, but not on the left ( $p_{\text{right}} < 0.001$  and  $p_{\text{left}}=0.090$ ). There were no significant changes in lung height for both sides, in hemidiaphragmatic height on the right as well as diaphragmatic area pre- and post-LVRS ( $p > 0.05$ ). Except for hemidiaphragmatic height on the left ( $p=0.039$ ), no significant differences were found on inspiration. Considering the 30% cut-off for treatment-benefit receiver operating curves (ROC) analysis indicated normalized total lung area as the most sensitive pre-operative outcome predictor for a 30% increase in FEV1% with a sensitivity of 86% and a specificity of 61% when height-normalized expiratory lung area is  $\geq 35793\text{mm}^2$ .

**Conclusion:** Pre-operative dMRI parameters can be used as additional outcome predictor for patient selection in LVRS. A height-normalized total lung area in expiration  $\geq 35793\text{mm}^2$  correlates with a 30% increase in FEV1%.

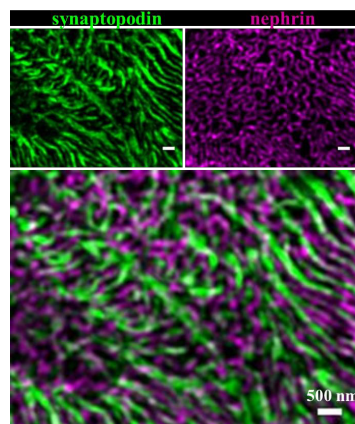
## Three-dimensional structured illumination microscopy as a novel diagnostic tool for nephrotic kidney diseases

Florian Siegerist, Nadine Artelt, Karlhans Endlich, Nicole Endlich

Department of Anatomy and Cell Biology, University Medicine Greifswald, Greifswald, Germany

Nephrotic syndrome is a severe kidney disease defined as the combination of proteinuria, hypalbuminemia, hyperlipidemia and edema. In nephrotic syndrome, a highly specialized cell of the kidney, the podocyte, is injured which leads to a loss of size selectivity of the renal filter with passage of high molecular weight protein into the primary urine. In nephrotic syndrome, podocyte foot process morphology changes to flat cellular protrusions which leads to rapid onset of proteinuria and subsequent scarring of the kidney which ultimately progresses to end stage renal disease. Since podocyte foot processes are around 250 nm in width, until now structural analysis could only be performed by electron microscopy. Unfortunately, electron microscopy requires time-consuming sample preparation and morphometry is error-prone due to physical sectioning of the sample which has led to prolonged time until diagnosis for patients and highly biased results in basic research.

Recently, superresolution fluorescence microscopy techniques have been developed which allow light microscopic resolution beyond *Abbe's* optical resolution limit of ~200 nm. Using three-dimensional structured illumination microscopy (3D-SIM) it is possible to at least double the resolution in all three directions. We hypothesized that 3D-SIM would allow the analysis of podocyte morphology and to diagnose foot process effacement. We used 3D-SIM



of renal tissue of human, murine and rat origin stained with antibodies against podocyte foot process proteins nephrin and synaptopodin. For automatic evaluation of podocyte morphology, we developed an ImageJ-based plugin.

In human samples, we measured a mean foot process width of  $0.249 \pm 0.68 \mu\text{m}$  in healthy, and  $0.675 \pm 0.246 \mu\text{m}$  in patients suffering from minimal change nephrotic syndrome. Additionally, we established the slit diaphragm density as a direct parameter for podocyte integrity.

Furthermore, we show that we can image characteristic changes in foot process morphology in the widely used animal models mice and rats and quantify podocyte foot process morphology in a genetic podocytopathy model induced by podocyte-

specific knockout of the actin-associated protein palladin.

Taken together, we have established a novel method which allows quick evaluation of podocyte morphology in a semi-automatized fashion. Including this technique into the diagnostic routine could effectively shorten the time of histopathological examination of patient biopsies and strengthen findings in basic renal research.

## A Soft Total Artificial Heart – 3D-Printing and Softness for More Physiological Implants

Nicholas H. Cohrs<sup>1</sup>, Anastasios Petrou<sup>2</sup>, Michael Loepfe<sup>1</sup>, Christoph T. Starck<sup>3</sup>, Marianne Schmid Daners<sup>2</sup>, Mirko Meboldt<sup>2</sup>, Volkmar Falk<sup>3</sup>, Wendelin J. Stark<sup>1</sup>

<sup>1</sup>Institute for Chemical and Bioengineering, ETH Zürich, Vladimir-Prelog-Weg 1, 8093 Zürich, Switzerland. <sup>2</sup>Product Development Group Zurich, ETH Zürich, Leonhardstrasse 21, 8092 Zürich, Switzerland. <sup>3</sup>Department for Cardiothoracic and Vascular Surgery, Deutsches Herzzentrum Berlin, Augustenburger Platz 1, 13353 Berlin, Germany.

Heart failure (HF) is one of the world's most significant diseases. It concerns more than 26 million people worldwide and reaches a share of 30% of all deaths. As the number of donor hearts is limited, the use of artificial blood pumps for HF patients is continuously increasing. Currently most implanted artificial hearts are so called ventricular assist devices (VAD), which support and relieve the weakened heart. In principle, these VADs are very basic pumps, which produce a continuous blood flow, rather than a physiological pulsatile one. This is intrinsically unnatural and possibly unhealthy, as the consequences of missing blood flow pulsatility remain unknown. In great contrast to the current focus on VAD technologies, we developed a total artificial heart using soft robotics principles, thus imitating the human heart in its form mechanical properties and function (i.e. by squeezing the blood). Using a 3D-printed mould and a lost-wax casting technique, it is possible to manufacture an entirely soft total artificial heart (sTAH), which is made of one single silicone elastomer monoblock and, in contrast to existing VADs, is completely soft [1, 2]. This technology, adapted from soft robotics aims at replicating the biomimetic motion of the human muscular system [1, 3, 4]. The sTAH mimics the human heart from a physiological and physical motion point of view, yielding pulsatile blood flow [1, 4]. Soft robotics technology could enable a first step towards personalized implants in artificial blood pump therapy [1]. Evaluation of the sTAH against physiological pre- and afterloads of the human circulatory system using a hybrid mock circulation [5] revealed a physiological pressure waveform, which is very similar to the one of the human heart. An aortic pulse pressure of 35 mmHg was reached, which is to our knowledge one of the most physiological pulse pressures, compared to any other artificial heart or VAD. Against a physiological afterload, the sTAH reaches a left ventricular flow of 2.2 L/min with a systolic/diastolic pressure of 71 to 36 mmHg. Vast improvements are feasible by adapting alternative elastomeric materials, optimization of the pneumatic drive and optimization of the chamber geometry.

- [1] N.H. Cohrs, A. Petrou, M. Loepfe, M. Yliruka, C.M. Schumacher, A.X. Kohll, C.T. Starck, M. Schmid Daners, M. Meboldt, V. Falk, W.J. Stark, *Artif Organs* **41**, 948-958, (2017).
- [2] C.M. Schumacher, M. Loepfe, R. Fuhrer, R.N. Grass, W.J. Stark, *RSC Adv* **4**, 16039-16042, (2014).
- [3] F. Ilievski, A.D. Mazzeo, R.F. Shepherd, X. Chen, G.M. Whitesides, *Angew Chem Int Ed* **123**, 1930-1935, (2011).
- [4] E.T. Roche, R. Wohlfarth, J.T.B. Overvelde, N.V. Vasilyev, F.A. Pigula, D.J. Mooney, K. Bertoldi, C.J. Walsh, *Adv Mater* **26**, 1200-1206, (2014).
- [5] G. Ochsner, R. Amacher, A. Amstutz, A. Plass, M. Schmid Daners, H. Tevaearai, S. Vandenbergh, M.J. Wilhelm, L. Guzzella, *IEEE Trans Biomed Eng* **60**, 507-516, (2013).



## Structural Characterization of Coronavirus Fusion Proteins

Alexandra C. Walls<sup>1</sup>, M. Alejandra Tortorici<sup>2,3</sup>, Xiaoli Xiong<sup>1</sup>, Brandon Frenz<sup>1</sup>, Joost Snijder<sup>1</sup>, Wentao Li<sup>1</sup>, Félix A. Rey<sup>2,3</sup>, Frank DiMaio<sup>1</sup>, Berend-Jan Bosch<sup>4</sup>, and David Veesler<sup>1\*</sup>

<sup>1</sup>Department of Biochemistry, University of Washington, Seattle, Washington, USA.

<sup>2</sup>Institut Pasteur, Unité de Virologie Structurale, Paris, France.

<sup>3</sup>CNRS UMR 3569 Virologie, Paris, France.

<sup>4</sup>Virology Division, Department of Infectious Diseases and Immunology, Faculty of Veterinary Medicine, Utrecht University, Utrecht, The Netherlands.

Two recent coronavirus epidemics, and the likelihood of future outbreaks, have urged the need to develop a vaccine against this family of pathogens. There are currently no approved vaccines or therapies for human infecting coronaviruses. Coronaviruses' deadly potential was first demonstrated in 2002 with the emergence of severe acute respiratory syndrome coronavirus and later in 2012 with Middle East respiratory syndrome coronavirus. There are four other known human-infecting coronaviruses, and many more coronaviruses that can infect and kill livestock and animals. Infection by these enveloped viruses is accomplished through membrane fusion mediated by the spike glycoprotein present on the surface of the virion. These spike proteins are trimeric in nature and are the main target of neutralizing antibodies during infection [1]. Initially the spike protein interacts with a host-cell receptor, and then undergoes a large conformational rearrangement to successfully mediate viral membrane fusion [2]. Following viral and host membrane fusion, the viral genetic material is disseminated into the host cell to propagate.

Leveraging recent advances in **cryo-electron microscopy** [3], we determined the structure of the first coronavirus spike protein in the pre-fusion conformation at near atomic resolution, detailing the molecular architecture and organization of this spike protein [4]. We have since characterized the same spike protein in the post-fusion state, mimicking how the protein would look following viral membrane fusion [5]. Comparison of these two states, one before viral infection and one following initial viral entry, allows for insights into the conformational trajectory these proteins undergo on the viral surface (Figure 1). These structures can be utilized as a framework for structure-guided inhibition of coronaviruses by targeting the conformational fusion transition upon viral entry. We have also used structure to uncover that the organization of the receptor binding subunit is drastically different between different coronaviruses, especially from distinct evolutionary families [4, 6, 7]. To further probe the structure of these viral fusion proteins, we have integrated these results with mass spectrometry to reveal the extensive glycan shield obstructing the protein surface, suggesting coronaviruses use both epitope masking with glycans and large conformational changes to evade the immune system of infected hosts [7]. From these structures, we defined a framework of viral entry and infection, paving the way for structure-guided design of inhibition strategies targeting coronaviruses.

References:

- [1] Du, L. *et al.* Nature Rev. Microbiol. 7, 226–236 (2009).  
 [2] Harrison, S.C. NSMB. 15: 690–698 (2008). [5] Walls, A.C. *et al.* PNAS. 114: 11157–11162. (2017).  
 [3] Li, X. *et al.* Nat. Methods. 10: 584–590 (2013). [6] Yuan, Y. *et al.* Nat. Commun. 8:15092 (2017).  
 [4] Walls, A. C. *et al.* Nature. 531: 114–117 (2016). [7] Walls, A.C. *et al.* NSMB. 10:899–905 (2016).

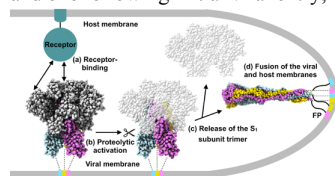


**Figure 1:** Conformational trajectory of the coronavirus spike protein from the pre-fusion structure as it exists on the viral surface to the post-fusion structure as it exists following viral entry and membrane fusion [5].

## Insight into Small Molecule Binding to the Neonatal Fc Receptor by X-ray Crystallography and 100 kHz Magic-Angle-Spinning NMR

Daniel Stöppler<sup>1</sup>, Alex Macpherson<sup>2</sup>, Susanne Smith-Penzel<sup>3</sup>, David Fox III<sup>4</sup>, Alastair Lawson<sup>2</sup>, Beat H. Meier<sup>3</sup>, and Hartmut Oschkinat<sup>1</sup>

<sup>1</sup> Leibniz-Institut für Molekulare Pharmakologie, Robert-Rössle-Str. 10, 13125 Berlin, Germany

<sup>2</sup> UCB Celltech, 208 Bath Road, Slough, Berkshire SL1 3WE, United Kingdom

<sup>3</sup> Laboratory of Physical Chemistry, ETH Zürich, Vladimir-Prelog-Weg 2, 8093 Zürich, Switzerland

<sup>4</sup> Beryllium Discovery, 3 Preston Ct, Bedford, MA 01730, USA

In drug design, a detailed characterization of structural changes in proteins upon ligand binding can help to further optimize compounds towards therapeutic interventions. In many cases, these structural alterations are distant from the small molecule binding site, providing a potential to achieve functional implications through allosteric effects. Such dynamic changes are often difficult to observe by static methods, i.e. X-ray crystallography, but can be monitored by NMR spectroscopy [1]. The latter, however, has size-limitations when investigating the protein backbone structure in solution-state. To overcome this, we herein establish an innovative approach employing ultrafast magic-angle-spinning (MAS) NMR on the soluble extra-cellular domain of the neonatal Fc receptor (FcR<sub>NECD</sub>), a crucial protein in regulation of Immunoglobulin G (IgG) and serum albumin catabolism. It is a clinically validated drug target for the treatment of autoimmune diseases caused by pathogenic antibodies, via the inhibition of its interaction with IgG [2]. In combination with computational methods, fragment screening, X-ray crystallography and other biophysical tools, we present the discovery of a small molecule that binds into an evolutionarily conserved cavity of FcR<sub>NECD</sub>. We provide a detailed structural characterization, to explore possibilities for refining the compound as an allosteric modulator. Proton-detected MAS NMR experiments on fully protonated [<sup>13</sup>C,<sup>15</sup>N]-labeled FcR<sub>NECD</sub> enabled us to observe ligand-induced structural changes for amino acid residues in the binding pocket and in remote regions of the protein. The introduced MAS NMR approach can be applied to a large variety of proteins to support structure-based drug discovery campaigns, facilitating the detection of allosteric effects.

[1] M. P. Williamson, Progress in Nuclear Magnetic Resonance Spectroscopy **73**, 1–16, (2013).

[2] Y. Wang, Z. Tian, D. Thirumalai, X. Zhang, Journal of Drug Targeting **22**, 269–278, (2014).



## Inferring whole-brain effective connectivity

Stefan Frässle<sup>1,+</sup>, Ekaterina I. Lomakina<sup>1,2,+</sup>, Lars Kasper<sup>1,3</sup>, Zina M. Manjaly<sup>4</sup>, Alex Leff<sup>5</sup>,  
Klaas P. Pruessmann<sup>3</sup>, Joachim M. Buhmann<sup>2</sup>, Klaas E. Stephan<sup>1,5</sup>

<sup>1</sup> Translational Neuromodeling Unit (TNU), Institute for Biomedical Engineering, University of Zurich & ETH Zurich, 8032 Zurich, Switzerland

<sup>2</sup> Department of Computer Science, ETH Zurich, 8032 Zurich, Switzerland

<sup>3</sup> Institute for Biomedical Engineering, ETH Zurich & University Zurich, 8092 Zurich, Switzerland

<sup>4</sup> Department of Neurology, Schulthess, 8008 Zurich, Switzerland

<sup>5</sup> Wellcome Trust Centre for Neuroimaging, University College London, London WC1N 3BG, United Kingdom

Developing whole-brain models that infer effective (directed) connectivity among neuronal populations from noninvasive neuroimaging data represents a holy grail for computational neuroscience and its application to clinically relevant questions [1, 2]. Specifically, whole-brain models of connectivity hold great promise to translate into “computational assays” since many psychiatric and neurological diseases are characterized by distributed abnormalities in large-scale networks, and whole-brain estimates of connectivity are emerging as powerful predictors for individual treatment response and clinical trajectory. We here developed a novel approach, *regression dynamic causal modeling* (rDCM) for functional magnetic resonance imaging (fMRI) data that enables whole-brain effective connectivity analyses [3].

First, we demonstrated in comprehensive simulations that rDCM can accurately recover known network architectures (i.e., the connections present in the data-generating model) and true connection strengths for large networks with up to 66 regions [3, 4]. We then applied rDCM to several empirical fMRI datasets. In particular, we showed that it is feasible to infer effective connection strengths from fMRI data using a network with more than 100 regions and 10,000 connections. Here, rDCM was applied to fMRI data from a simple motor paradigm (visually paced fist closings) (Fig. 1A). Model inversion resulted in a sparse graph with biologically plausible connectivity (Fig. 1B, left) and driving input patterns (Fig. 1B, right): we observed pronounced driving inputs to and functional integration among motor regions (precentral, SMA, cerebellum), visual regions (cuneus, occipital), regions associated with the somatosensory and proprioceptive aspects of the task which are essential for visuomotor integration (postcentral, parietal), and frontal regions engaging in top-down control. The inferred effective connectivity pattern and its sparseness become most apparent when visualized as a connectogram (Fig. 1C) or projected onto the whole-brain volume (Fig. 1D). Notably, inversion of this whole-brain model was computationally highly efficient and took only 10 minutes on a standard laptop, suggesting that our approach may scale to even larger networks.

Regression DCM allows one to infer effective (directed) connectivity, with connection-specific estimates, in whole-brain networks from noninvasive fMRI data. We anticipate that rDCM will offer tremendous opportunities for clinical applications, such as whole-brain phenotyping of patients, as well as prediction of clinical trajectory and treatment success [2]. In a next step, we therefore aim to apply rDCM to patient datasets (e.g., [5]) to demonstrate the clinical utility of our approach.

## Tired of working: The impact of effortful exertion on brain and behaviour

Tanja Müller, Masud Husain, Matthew Apps

Department of Experimental Psychology, University of Oxford  
Woodstock Road, Oxford OX2 6GG, United Kingdom

Fatigue – a feeling of exhaustion arising from effortful exertion – is a highly prevalent and debilitating symptom across a broad range of neurological and psychiatric conditions. In a milder form, it is also frequently reported in otherwise healthy people [1,2]. During physically or mentally demanding tasks, fatigue increases over time and can lead to impaired accuracy and vigour of behaviours, but in healthy people fatigue usually decreases by taking a rest. Psychological theories suggest that rather than affecting performance directly, fatigue impacts on motivation, reducing the willingness to exert effort over time [3-5]. However, to date, the psychological processes and brain systems that underpin fatigue and its impact on subsequent motivation are poorly understood. Using an effort-based decision-making paradigm in combination with mathematical modelling and brain imaging (functional magnetic resonance imaging [fMRI]) we investigated the effects of effortful exertion on subsequent effort-based decisions in healthy people to understand more about the processes in the brain that underlie fatigue. Participants ( $N = 32$ ) made a series of choices between two alternatives: a rest option for a low reward (1 credit) or a work option, requiring the exertion of one of three levels of grip force (30-48% of their maximal grip strength), for one of three higher amounts of reward (6-10 credits). Mathematical modelling revealed that choices of higher effort work options declined over trials as a function of (i) the effort previously accumulated over the course of the whole task and (ii) a recoverable component that increases after trials of effortful exertion and is restored by trials of resting. fMRI analysis revealed neural activity in sensorimotor and prefrontal brain areas to play a crucial role in the modulation of effort-based decision-making by previous exertion or rest. These results provide insights into the mechanisms underlying momentary fatigue and the dynamics of motivation. Moreover, the computational framework may provide a new way of probing fatigue and impaired motivation in clinical disorders such as for example Parkinson's Disease.

[1] A. Chaudhuri & P. O. Behan, *Lancet* **363**, 978–988 (2004).

[2] W. Cullen, Y. Kearney, & G. Bury, *Irish Journal of Medical Science* **171**, 10–12 (2002).

[3] M. A. S. Boksem & M. Tops, *Brain Research Reviews* **59**, 125–139 (2008).

[4] R. Kurzban, A. Duckworth, J. W. Kable, & J. Myers, *Behavioral and Brain Sciences* **36**, 661–679 (2013).

[5] M. Tanaka & Y. Watanabe, *Neuroscience & Biobehavioral Reviews* **36**, 727–734 (2012).

## Investigation of Sleep/Wake Regulatory Mechanisms by Analysis of the *Sik3* Gene Identified Through Forward Genetics

Takato Honda<sup>1,2,3</sup>, Tomoyuki Fujiyama<sup>1</sup>, Chika Miyoshi<sup>1</sup>,  
Hiromasa Funato<sup>1</sup> and Masashi Yanagisawa<sup>1</sup>

1. International Institute for Integrative Sleep Medicine (WPI-IIS), University of Tsukuba, Tsukuba, 305-8575, Japan
2. Japan Society for the Promotion of Science (JSPS) Overseas Research Fellow, Tokyo, 102-0083, Japan
3. The Picower Institute for Learning and Memory, Massachusetts Institute of Technology (MIT), Cambridge, MA 02139, USA

As a mystery of sleep biology, the neuronal substrate for “sleepiness” and the molecular mechanisms determining daily sleep amounts and sleep need have been unveiled. A simple model animal such as fruit fly *Drosophila* has been contributed to the understanding of neural circuit basis of various behaviors [1, 2]. However, the locomotor-based criteria of sleep in invertebrates have a difficulty to distinguish between the states of quiet wakefulness and actual sleep. To achieve a breakthrough on this issue and find the novel genes regulating sleep/wake behaviors, we have initiated a large-scale forward genetic screen of sleep/wake phenotype in mice, based on true somnographic (EEG/EMG) measurements, which are the gold standard in mammalian sleep/wake assessment including human. To date, we have screened > 8,000 heterozygous ENU-mutagenized mice and established multiple pedigrees exhibiting heritable and specific sleep/wake abnormalities. Through the forward genetic analysis of sleep in randomly mutagenized mice, we identified a splicing mutation in the *Sik3* gene (*Sleepy* mutation) that increases non-REM sleep (NREMS) and sleep need [3]. The *Sleepy* mutation deletes an in-frame exon encompassing S551 residue, an evolutionally conserved PKA recognition site in SIK3. Thus, we hypothesized that S551 has an essential role for the regulation of daily sleep amount and sleep need. To examine this hypothesis, we generated mutant mice with single amino acid substitutions, S551A (*S551A* mutant) and S551D (*S551D* mutant), by using the CRISPR/Cas9 system. As a result, *S551A* and *S551D* mutants exhibited the markedly increased NREMS amount and inherently increased baseline sleep need, owing to the increased duration of individual NREMS episodes and higher densities of EEG slow-wave activity during NREMS [4]. At the molecular level, deletion or mutation at SIK3 S551 reduced PKA recognition and abolished 14-3-3 binding. These results suggest that the existence of S551 in *Sik3* gene and its signaling pathway including PKA, SIK3 and 14-3-3 may have a key role on sleep/wake regulation in normal physiological condition. Importantly, S551 SIK3 is evolutionally conserved as a PKA phosphorylation site from nematodes, fruit flies, mice to humans. These findings provide landmark information about the novel sleep/wake regulatory mechanisms by connecting the intracellular signaling pathway to the dynamic *in vivo* sleep/wake behaviors.

- [1] T. Honda, K. Furukubo-Tokunaga et al, *Scientific Reports* 4, 4798 (2014)
- [2] T. Honda, K. Furukubo-Tokunaga et al, *Frontiers in Behavioral Neuroscience* 10, 137 (2016)
- [3] H. Funato, T. Honda, M. Yanagisawa et al, *Nature* 539, 378–383 (2016)
- [4] T. Honda, H. Funato, M. Yanagisawa et al, *PNAS*, in press (2018)

## Functional impairment of cortical astrocytes in ALS-transgenic mice

Maximilian Bauer<sup>1</sup>, Melisa Suljkanovic<sup>1</sup> and Sabine Liebscher<sup>1</sup>


<sup>1</sup>Emmy Noether/Clinician Scientist Group, Institute of Clinical Neuroimmunology, Klinikum der Universität München and BioMedical Center, Ludwig-Maximilians-University Munich, Martinsried, Germany

Amyotrophic lateral sclerosis (ALS), the most common adult-onset motor neuron disease, is a fatal disorder caused by the progressive degeneration of upper and lower motor neurons. Intriguingly, there is *in vitro* and *in vivo* evidence that dysfunction of astrocytes bearing ALS-associated mutations alone can be sufficient to cause selective motor neuron death. We hypothesized that astrocytes are compromised in their physiological function during the course of the disease, which might fuel or even trigger motor neuron degeneration.

Despite being electrically silent, astrocytes can display calcium signals of varying forms, ranging from subcellular microdomain activity to global waves spreading over long distances. Moreover, one recently discovered functional response property of cortical astrocytes are large calcium signals driven by the locomotion of the animal. In order to test whether physiological response properties of cortical astrocytes are impaired during the course of the disease, we recorded calcium signals in behaving ALS-transgenic mice (expressing the human superoxide dismutase 1 (SOD1) gene containing the G93A mutation) by means of two-photon imaging. We employed the genetically encoded calcium indicator GCaMP6, selectively expressed in astrocytes, while mice were free to run on a spherical treadmill.

We found that the marked locomotion-associated calcium responses, typically seen in astrocytes in the motor cortex (M1) of WT mice were disturbed in ALS-transgenic mice in multiple ways: First, astrocytes responded less vigorously, as seen e.g. in a reduced population response. Furthermore, astrocytes responded less reliable to running events, as shown by an increase in the fraction of non-responded running epochs (failure rate) and an overall weaker correlation of the astrocytic calcium signal to the running velocity. To probe how well the astrocyte population encodes information on the actual running velocity, we implemented a machine learning algorithm to decode running speed based on calcium activity. Corroborating our results, we found a poorer coding accuracy in ALS-transgenic mice. All above mentioned effects were observed both in layer 1 and layer 2/3 of M1. Interestingly, we witnessed functional impairments of astrocytes not only in the motor cortex (M1), the site typically affected in ALS, but moreover we found evidence for similar alterations within the primary visual cortex (V1), a non-affected control area, indicating that astrocytes might be globally affected in the disease.

Taken together, our results add further credence to the notion of pronounced functional alterations of cortical astrocytes in ALS. Future studies are needed to unravel the underlying molecular mechanisms, the time course, regional specificity and importantly the impact of such functional alterations seen in astrocytes on neuronal health.

The image features a large, abstract graphic on the left side composed of numerous thin, green, wavy lines that create a sense of movement and depth. On the right side, there is a black and white photograph of a person from the chest up, wearing a wide-brimmed hat with a dark band and a light-colored, textured garment. The person's face is partially obscured by the hat and the abstract lines.

Council for the Lindau Nobel Laureate Meetings  
Foundation Lindau Nobel Laureate Meetings

Alfred-Nobel-Platz 1  
88131 Lindau  
Germany

[www.lindau-nobel.org](http://www.lindau-nobel.org)